MAUSAM, **76**, 4 (October 2025), 1079-1094

MAUSAM

DOI: https://doi.org/10.54302/mausam.v76i4.7107
Homepage: https://mausamjournal.imd.gov.in/index.php/MAUSAM

UDC No. 502.3:613.15(540.27)

Elemental characteristics of atmospheric aerosols using Raman spectroscopy: a case study from Doon valley during Covid-19 pandemic

AMAN SHRIVAS[1#, 2], CHHAVI PANT PANDEY[1, 2*], ABHISHEK THAKUR [1$, 2],

PARAKH SAHU [1, 2!] and SWARNENDU ROY [1, 2^]

[1]Wadia Institute of Himalayan Geology, Dehradun, India

([#]amanshrivas@wihg.res.in, [$]abhishekthakur@wihg.res.in)

[2]Academy of Scientific and Innovative Research, Ghaziabad, India

([!]parakhsahu@wihg.res.in, ^Swarnendu@wihg.res.in)

(*Received 9 May 2025, Accepted 8 September 2025*)

***Corresponding author's email: chhavi@wihg.res.in**

सार – यह अध्ययन कोविड-19 लॉकडाउन अवधि (अप्रैल से सितंबर 2020) के दौरान वाडिया हिमालय भूविज्ञान संस्थान, देहरादून परिसर से एकत्रित कुल निलंबित कणों (TSP) वायुविलय की रमन स्पेक्ट्रोस्कोपिक जाँच प्रस्तुत करता है। लॉकडाउन ने एक दुर्लभ निम्न-उत्सर्जन वायुमंडलीय स्थिति उत्पन्न की, जिसने सामान्य मानवजनित हस्तक्षेप की अनुपस्थिति में परिवेशी वायुविलय की रासायनिक प्रकृति की जाँच करने का एक आदर्श अवसर प्रदान किया। एथेलोमीटर AE51 की पॉलीटेट्राफ्लुओरोएथिलीन (PTFE) फ़िल्टर पट्टी का विश्लेषण करने के लिए रमन माइक्रो-स्पेक्ट्रोस्कोपी का उपयोग किया गया, जिससे उनके कार्बनयुक्त और कार्बनिक संघटन के बारे में आणविक स्तर की जानकारी प्राप्त हुई। मॉनसून-पूर्व महीनों (अप्रैल-मई) के दौरान एकत्रित स्पेक्ट्रा में सुविभेदित D (~1350 cm^{-1}) और G (~1580 cm^{-1}) बैंडों का प्रभुत्व था, जो दहन स्रोतों से अव्यवस्थित और ग्रेफाइटिक ब्लैक कार्बन (BC) की उपस्थिति का संकेत देते हैं। इसके विपरीत, मॉनसून ऋतु (जून-अगस्त) के स्पेक्ट्रा में ऑक्सीजन युक्त और एलिफैटिक कार्बनिक यौगिकों के बढ़े हुए योगदान के साथ विस्तृत बैंड दिखाई दिए, जैसा कि 1700-3100 सेमी$^{-1}$ रेंज में चोटियों से प्रमाणित होता है। ये विशेषताएँ उच्च आर्द्रता के तहत जलीय-प्रावस्था और प्रकाश-रासायनिक आयुवृद्धि प्रक्रियाओं के माध्यम से द्वितीयक कार्बनिक वायुविलय (SOA) निर्माण को दर्शाती हैं। सितंबर तक, मॉनसून पूर्व परिस्थितियों के आगमन के साथ, दहन से उत्पन्न कार्बन संकेत, पुराने ऑक्सीकृत कार्बनिक पदार्थों के साथ मिश्रित होकर, फिर से उभरने लगे। विभिन्न ऋतुओं में रमन वर्णक्रमीय विकास, वायुविलय संरचना पर मौसम विज्ञान और उत्सर्जन गतिकी के प्रभाव को प्रकट करता है। मॉनसून-पूर्व वायुविलय में प्राथमिक कार्बन डाइऑक्साइड (BC), मॉनसून वायुविलय में वृद्ध कार्बनिक पदार्थ, और मॉनसून-पश्चात वायुविलय में दोनों का संयोजन पाया गया। यह कार्य वायुविलय की आणविक फिंगरप्रिंटिंग के लिए रमन स्पेक्ट्रोस्कोपी की उपयोगिता पर प्रकाश डालता है और हिमालय की तलहटी में वायुविलय की आयुवृद्धि और स्रोत परिवर्तन प्रक्रियाओं को समझने के लिए एक मौसमी संदर्भ प्रदान करता है।

ABSTRACT. This study presents a Raman spectroscopic investigation of total suspended particles (TSP) collected from Wadia Institute of Himalayan Geology, Dehradun Campus, during the COVID-19 lockdown period (April to September 2020). The lockdown created a rare low-emission atmospheric condition, offering an ideal opportunity to examine the chemical nature of ambient aerosols in the absence of usual anthropogenic interference. Raman micro-spectroscopy was used to analyze the Polytetrafluoroethylene (PTFE) filter strip of aethalometer AE51, providing molecular-level insights into their carbonaceous and organic composition. Spectra collected during the pre-monsoon months (April-May) were dominated by well-resolved D (~1350 cm^{-1}) and G (~1580 cm^{-1}) bands, indicating the presence of disordered and graphitic black carbon (BC) from combustion sources. In contrast, spectra from the monsoon months (June-August) exhibited broadened bands with enhanced contributions from oxygenated and aliphatic organic compounds, as evidenced by peaks in the 1700-3100 cm^{-1} range. These features reflect secondary organic aerosol (SOA) formation through aqueous-phase and photochemical aging processes under high humidity. By September, the onset of post-monsoon conditions led to a resurgence of combustion-derived carbon signatures, mixed with aged oxidized organics. The Raman spectral evolution across seasons reveals the influence of meteorology and emission dynamics on aerosol composition. Pre-monsoon aerosols were dominated by primary BC, monsoon aerosols by aged organics, and post-monsoon aerosols by a

combination of both. This work highlights the utility of Raman spectroscopy for molecular fingerprinting of aerosols and provides a seasonal reference for understanding aerosol aging and source transformation processes in the Himalayan foothills.

Key words – Atmospheric aerosols, Black carbon, Raman spectroscopy, COVID-19.

1. Introduction

Aerosol particles are essential components of the atmosphere that influence both climate and human health (Pöschl, 2005). The sources of these airborne particles, *i.e.*, aerosols, are diverse and include both natural (soil dust, sea spray, volcanic emissions, and biogenic activities) and man-made (fossil fuel combustion, vehicle emissions, industrial processes, and biomass burning) activities (Perumpully & Gautam, 2024) and references therein. The airborne particles can travel to great distances, interact with atmospheric constituents, and can change chemical composition once they are suspended in the atmosphere (Chin *et al.*, 2015). The environment and public health may be seriously threatened by the complex mixture of organic compounds, inorganic salts, transition metals, and carbonaceous particles like black carbon (BC) and organic carbon (OC) that are frequently carried by aerosols, hazardous are trace metals such as cadmium (Cd), lead (Pb) and zinc (Zn), which are known to have toxic effects even at low concentrations and to contribute to oxidative stress, respiratory inflammation, and long-term systemic health problems. (Jacobson & Hansson, 2000) and references therein.

Fine particulate matter (PM2.5 and smaller or PM) is of particular concern because it has the ability to penetrate deep into the respiratory tract and can easily enter the bloodstream, leading to cardiovascular, neurological, and pulmonary diseases (Sangkham *et al.*, 2024) and references therein. In addition to their effects on human health, aerosols participate in heterogeneous chemical reactions, modify cloud microphysics, and can affect the Earth's radiative balance by absorbing and scattering solar radiation. (Buckner *et al.*, 2016; S *et al.*, 2013). In the ecologically delicate area such as the Himalayan region, these effects are intensified and can result in changes to regional snow darkening, hydrological cycles and glacier retreat (Ramachandran *et al.*, 2023; Sharma *et al.*, 2022).

Carbonaceous aerosols, made up of a significant fraction of atmospheric PM, include elemental and organic carbon. These particles are considered the most crucial for surface-atmosphere energy interactions, light absorption and cloud condensation. They are essential indicators for tracking emissions from combustion sources like diesel engines, coal burning, and biomass use because of their unique and specific optical characteristics (Contini *et al.*, 2018; Ramachandran *et al.*, 2023; Sharma *et al.*, 2022; Yan *et al.*, 2019). For optical observation-based reporting of BC, equivalent black carbon (eBC) is used (Petzold *et al.*, 2013; Watson *et al.*, 2005). While eBC measures the total amount of refractory carbon, graphitic soot particularly refers to particles of structurally organized carbon that exhibit enhanced light absorption and distinct aging characteristics. (Sadezky *et al.*, 2005).

Aerosol pollution in climate-sensitive and densely populated areas like the Himalayan Doon Valley raises serious environmental and health concerns, especially considering the lack of instrumental air monitoring networks in the area. Utilizing the Microaeth AE51 instrument, the ambient aerosol samples were collected for this investigation (Cheng & Lin, 2013). Advanced Raman spectroscopy (RS) of carbonaceous particles gathered on Teflon filter strips was used to carefully analyze the structural characteristics and chemical signature of suspended carbon materials. Identifying characteristic peaks via RS improves knowledge of particle behaviors and environmental effects (Doughty & Hill, 2020; Estefany *et al.*, 2023). This in-situ chemical characterization is essential for identifying the monthly and seasonal fluctuations in particle composition, particularly in areas like Dehradun, where pollution problems are escalating due to growing urbanization (Ferrari & Robertson, 2000; Ivleva *et al.*, 2007; Long, 2004). This thorough approach to air quality monitoring emphasizes the necessity of continuing studies to address the negative effects of pollution on the environment and human health in areas like Dehradun that are fast becoming more urbanized. This study uses rigorous statistical techniques, such as ANOVA, to give strong evidence of temporal fluctuations, which aids in identifying the sources of pollutants and clarifying their effects on the environment and public health. The main objective of this study is to provide a thorough investigation of the chemical makeup and evolution of aerosols in the Doon Valley. This will help to establish the scientific foundation for policy interventions aimed at managing air quality and protecting the environment in the foothills of the Himalaya.

2. Data and methodology

2.1. *Study area*

Dehradun, the capital of the Indian state of Uttarakhand, is located in the Doon Valley along the Himalayan foothills, between the Siwalik Hills to the south and the Lesser Himalaya to the north, forming a

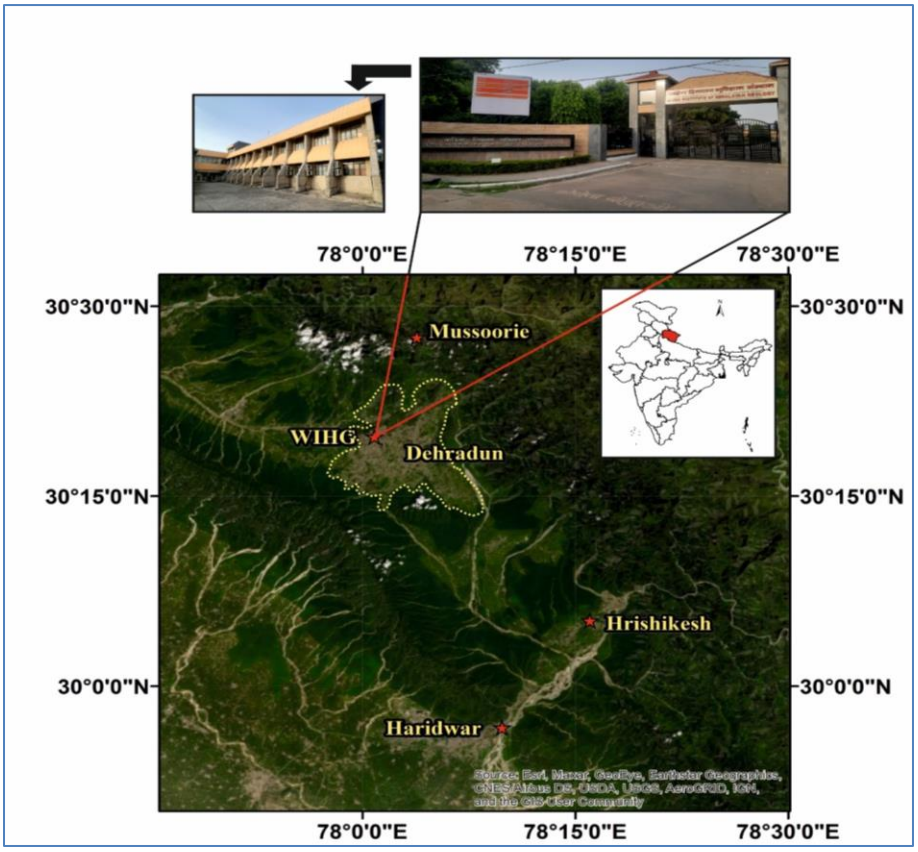

Fig. 1. Aerial view of Doon valley and its vicinity (dotted yellow lines represent the Dehradun city boundaries), the inset image represents the sampling area

valley that is ideal for urban growth and settlements (Panikkar & Subramanyan, 1996; Sinha & Sinha, 2016). Fig. 1 depicts the aerial view of Doon Valley, and the inset image shows the study area.

The city has a population of approximately 1.2 million, and it has experienced rapid urbanization and industrial growth that has resulted in a considerable increase in atmospheric pollutants from different sources like transportation, industrial, domestic, and construction activities (Government of Uttarakhand, 2018; Deep *et al.*, 2019; Dhankar *et al.*, 2024). Its valley setting often traps pollutants, causing severe degradation of air quality, especially from late October through winter. Major outdoor air pollutants include aerosols and hazardous gases from diverse anthropogenic sources, while indoor air pollution is largely attributed to the burning of biomass, waste, and coal (Pandey & Negi, 2022). During the COVID-19 lockdown, the significant reduction in human activities provided a rare opportunity to conduct chemical characterization of Total Suspended Particles (TSPs) under minimal anthropogenic influence. This study was conducted at the WIHG campus located in Dehradun. Although the observations were made in a clean setting within the institute's premises, the premises itself is located in the city Centre, surrounded by dense human settlement and heavy traffic.

2.2. *Climate and meteorology*

Doon Valley exhibits a temperate climate with significant seasonal variations influenced by its topography, where winters are relatively cold (5.2-23.4 °C) and summers can reach up to 44 °C during brief heatwave periods. (Singh *et al.*, 2013) documented a notable warming trend with annual temperatures increasing by 0.38 - 0.49 °C between 1967 and 2007, and increased rapidly since Dehradun became Uttarakhand's capital. Rainfall is predominantly concentrated during monsoon months (June-September), with July-August being the wettest, while the city's climatic variability is highlighted by elevation differences and proximity to the high-altitude Mussoorie hills (Piyoosh & Ghosh, 2016). Recent analyses reveal contrasting temperature trends with monsoon maximum temperatures declining by 1.99 °C (1981-2023), while post-monsoon minimum temperatures have risen by 2.85 °C during the same period (Mani, A.; Kumari, M.; Badola, 2024).

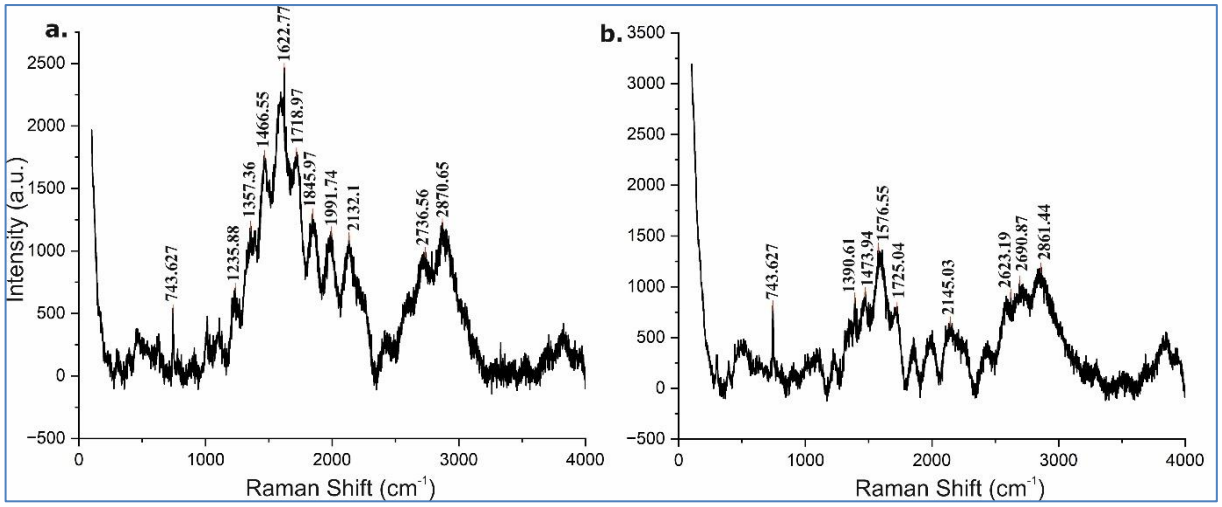

Figs. 2(a&b). Raman spectra of blank AE51 filter tape showing characteristic peaks of polytetrafluoroethylene (PTFE) and minor background features

2.3. *Data acquisition*

The AE-51 is conventionally used for real-time BC monitoring via optical attenuation at 880 nm; it functioned exclusively as a reliable field sampler due to its compact design, integrated pump, and flow stabilization system operating at 100 ml min^{-1} (Cheng & Lin, 2013; Sedlacek, 2016). Although this instrument is primarily used for optical characterization of BC aerosols, in this study it was used as a particulate sampler due to its chemically inert Teflon filter medium, stable flow control and low Raman background interference (Watson *et al.*, 1998). Sampling was conducted from April to September 2020, encompassing pre-monsoon and monsoon periods. RS measurements were performed at the WIHG, Dehradun, using the LabRAM HR Raman spectrometer (Horiba Jobin Yvon), equipped with a 532 nm argon-ion laser and a CCD detector cooled to –70 °C to enhance sensitivity. The spectrometer was calibrated using synthetic silica (520.5 cm^{-1}) and graphite standards, while laser exposure times (1–150 s) and power were carefully adjusted to prevent sample degradation. A laser spot diameter of ~2 µm enabled analysis of fine particulate structures, and spectral resolution was achieved using a grating of 600 grooves/mm, suitable for resolving key Raman-active modes in carbonaceous and mineral particles. RS has been widely used to characterize the chemical fingerprints of soot, mineral dust, and organic compounds in ambient aerosols (Ivleva *et al.*, 2007; Sobanska *et al.*, 2014). Its high specificity to molecular structure allows detailed analysis of complex TSP matrices, aiding in the interpretation of aerosol sources and transformation processes under different environmental conditions, such as those encountered during the COVID-19 lockdown (Ivleva *et al.*, 2007; Rao, 1978; Sobanska *et al.*, 2014).

3. Result and analysis

Atmospheric aerosols are complex mixtures of solid and liquid particles suspended in the air, playing a significant role in air quality, climate forcing, and human health (Sadezky *et al.*, 2005). Among these, BC, a primary component of combustion-derived aerosols, is particularly important due to its strong light-absorbing properties and influence on radiative balance (Bond *et al.*, 2013). Understanding the chemical and structural characteristics of such aerosols is essential for evaluating their atmospheric behavior and climate impact (Shrivas & Pandey, 2024). RS is a powerful method to understand the molecular composition of aerosols, particularly distinguishing between disordered, amorphous and graphitic carbon and identifying oxidized organic species (Ivleva *et al.*, 2007; Sadezky *et al.*, 2005). The results presented here provide spectral insights into the monthly variability in aerosol composition during the COVID-19 lockdown period, with emphasis on carbonaceous content and its chemical evolution.

3.1. *Blank filter*

The RS of the blank AE51 filter tape (Figs. 2 (a&b)), mainly composed of Teflon-coated borosilicate glass fiber (T60), reveals sharp vibrational characteristics corresponding to the materials used in the filter substrate. The most prominent peak observed around 743 cm^{-1} corresponds to the bending vibrations of CF_2 groups, which is a characteristic feature of PTFE, commonly known as Teflon (Asrafali *et al.*, 2024). This aligns with previously reported Raman spectra on fluoropolymers, where strong and sharp peaks in this region are attributed to symmetric CF_2 deformations (Li *et al.*, 2018; Zhou *et al.*, 2014).

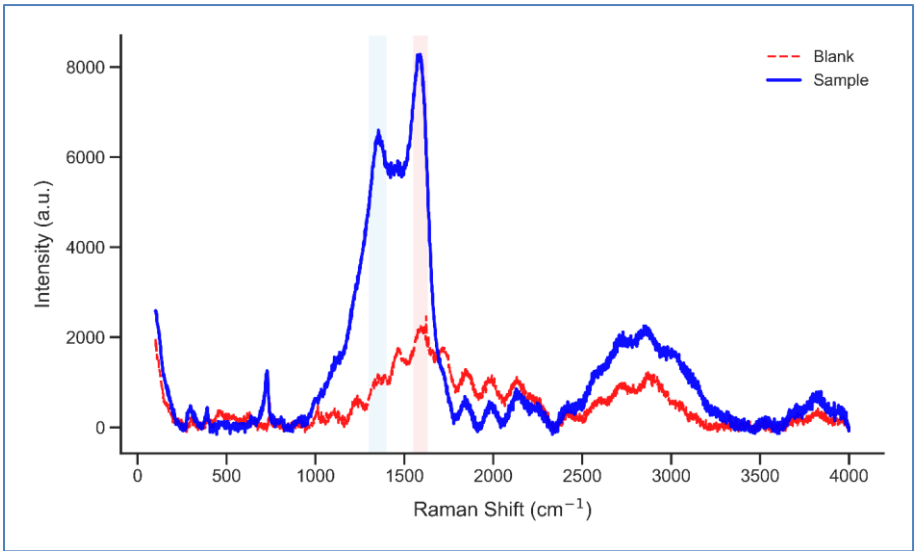

Fig. 3. Overlay of blank (substrate) vs sample Raman shift spectra depicting negligible substrate contributions to the sample peaks

A feature in the range of 1235-1390 cm^{-1} is also visible and can be attributed to asymmetric stretching vibrations of the CF_2 units in the Teflon structure. These vibrations are innate to the polymer backbone and act as spectral signatures for PTFE.

Furthermore, the less intense peaks between 1320 and 1465 cm^{-1} may arise from minor surface contaminants or weak Raman signals from the underlying borosilicate glass fiber. The borosilicate matrix, primarily composed of SiO_2, can exhibit weak and broad Raman bands due to Si–O–Si bending vibrations, often appearing in this spectral region (Mcmillan & Wolf, 1990; McMillan & Piriou, 1983). A notable peak around 1725 cm^{-1} could indicate the presence of trace organic compounds such as carbonyl-containing groups (*e.g*., esters or ketones), possibly introduced during the filter manufacturing or handling process. Furthermore, weak bands near 2145 cm^{-1} and in the high wavenumber region (2600–2900 cm^{-1}) may arise from overtones or combinations, or from marginal hydrocarbon contamination. Such background spectral characterization is essential to distinguish between filter-originated signals and those from actual aerosol particle constituents when performing micro-Raman analysis of ambient samples.

As seen in Fig. 3, the overlay of blank substrate (red dashed line) and aerosol sample (blue solid line) RS clearly demonstrates that the intense D and G bands at ~1500-1600 cm^{-1} and the broad organic features at ~2500-3000 cm^{-1} originate entirely from the collected aerosol particles rather than the filter substrate. The blank spectrum shows only a minimal background signal with negligible intensity compared to the sample, confirming that all major spectral features represent genuine atmospheric aerosol components. This comparison validates that the observed carbonaceous and organic signatures are not artifacts from the Teflon filter substrate.

3.2. *Month-wise detailed analysis*

3.2.1. April

The Raman spectra obtained from aerosol samples collected in April 2020 during the first COVID-19 lockdown over the WIHG campus in Dehradun (Figs. 4 (a-e)) reveal a complex matrix of carbonaceous and organic molecular signatures, indicative of reduced anthropogenic activity and the resultant atmospheric transformations. All five spectra (a-e) display two prominent carbon bands, the D-band (~1350 cm^{-1}) and the G-band (~1580-1600 cm^{-1}), which are characteristic of disordered and graphitic sp^2 carbon structures, respectively (Ferrari & Robertson, 2000; Sadezky *et al*., 2005). These bands confirm the presence of BC and graphitic soot in the collected aerosol particles, even during significantly reduced emissions.

Spectra (a) and (b) exhibit secondary peaks around ~1710 cm^{-1} and ~2900 cm^{-1}, corresponding to carbonyl C=O stretching vibrations and C-H stretching modes, respectively (Movasaghi *et al.*, 2007). These features suggest contributions from oxidized organic aerosols or SOAs, likely formed via atmospheric photochemical aging under cleaner lockdown conditions (Jimenez *et al.*, 2009). The relatively strong intensity of the C-H symmetric/asymmetric stretching peaks (2800–3000 cm^{-1}) across most spectra also highlights the presence of

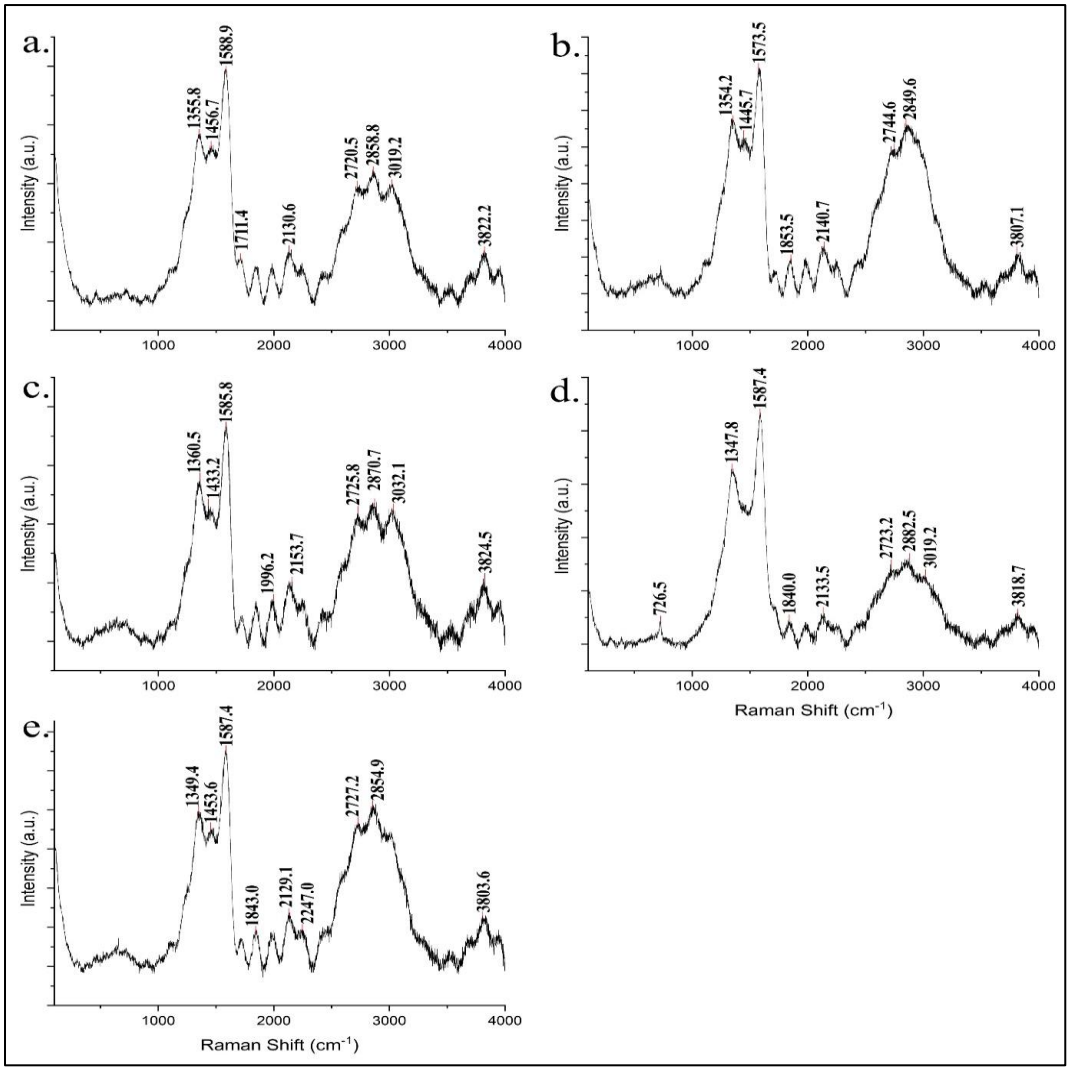

Figs. 4(a-e). Raman spectra (a-e) of aerosol samples collected during April 2020 from WIHG Campus, Dehradun

aliphatic hydrocarbons, probably emitted from residual biomass burning or household combustion sources (Chandrakala *et al.*, 2024; Van Poppel *et al.*, 2023; Verma & Kamyotra, 2021). Peaks in the region of 720-760 cm^{-1} (visible in spectra d and e) may be attributed to out-of-plane C-H bending modes, commonly associated with polycyclic aromatic hydrocarbons (PAHs) or ring-breathing modes in substituted benzenes (Long, 2004; Tuinstra F & Koenig Jl, 1970).

The diversity of Raman shifts and the relative intensities among Figs. 4 (a-e) suggest temporal variability in source composition and atmospheric processing. Compared to pre-lockdown literature reports, the reduced graphitic-to-disordered (G/D) intensity ratio observed in some spectra implies decreased fossil fuel combustion and increased contribution from low-temperature combustion or non-combustion organic sources (Liu *et al.*, 2016; C. P. Pandey & Negi, 2022; K. Pandey *et al.*, 2024). These spectral features provide a molecular-level snapshot of ambient PM composition during a rare low-emission period and offer a unique contrast to typical urban aerosol conditions.

3.2.2. *May*

The investigation of the RS of aerosol samples collected in May 2020, as seen in Figs. 5 (a-e), depicts a complex chemical mixture typical of combined carbon-based and organic materials of pre-monsoon conditions. The most prominent peak is a strong band near ~1350 cm^{-1}, indicating disorder in carbon structures, often associated with freshly emitted BC or soot from combustion processes such as vehicular emissions or

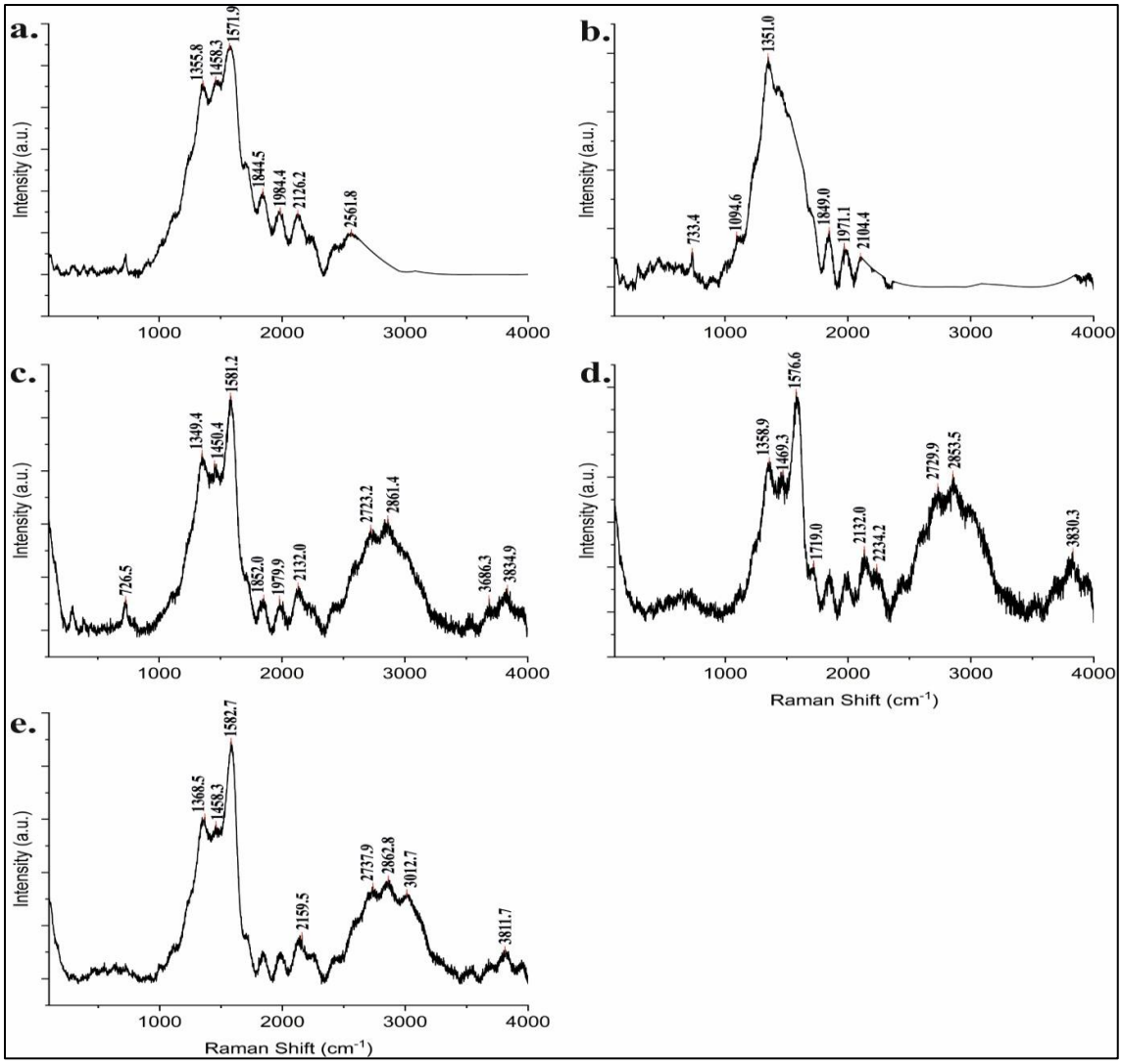

Figs. 5(a-e). Raman spectra (a-e) of aerosol samples collected during May 2020 from WIHG Campus, Dehradun

biomass burning (Ferrari & Robertson, 2000; Sadezky *et al.,* 2005). Unlike typical soot spectra, however, several samples notably lack a clear G-band (~1580 cm^{-1}), indicating the presence of more amorphous carbon or primary particles with minimal atmospheric aging. At the same time, distinct peaks observed around ~1750 cm^{-1} suggest the presence of C=O functional groups, which are indicative of oxidized organic compounds such as SOAs or humic-like substances (HULIS) (Liu *et al.,* 2016; Long, 2004). Furthermore, the broad and often overlapping bands between ~2500 and 3100 cm^{-1}, especially near ~2850-2930 cm^{-1}, reflect aliphatic C–H stretching vibrations, often associated with fossil-fuel-related emissions and biogenic organics (Ivleva *et al.,* 2007; Movasaghi *et al.,* 2007). Collectively, these spectrum characteristics investigation leads to a complex atmospheric mixture in May 2020 that is compatible with dry, sunny, and polluted pre-monsoon conditions in the Indo-Gangetic Plain and nearby Himalayan foothills. This mixture is characterized by primary emissions as well as indications of photochemical aging. The spectral variation in samples indicates both spatial and temporal heterogeneity in aerosol sources and atmospheric transformation processes.

3.2.3. *June*

The Raman spectra of aerosol samples collected in June 2020 (Figs. 6 (a-f)) reflect the characteristics of highly carbonaceous materials and oxidized organic constituents. All six (Figs. 6 (a-f)) consistently show strong D (~1330–1350 cm^{-1}) and G (~1550–1580 cm^{-1}) bands, indicating the predominance of disordered (amorphous) and graphitic sp^2 - hybridized carbon,

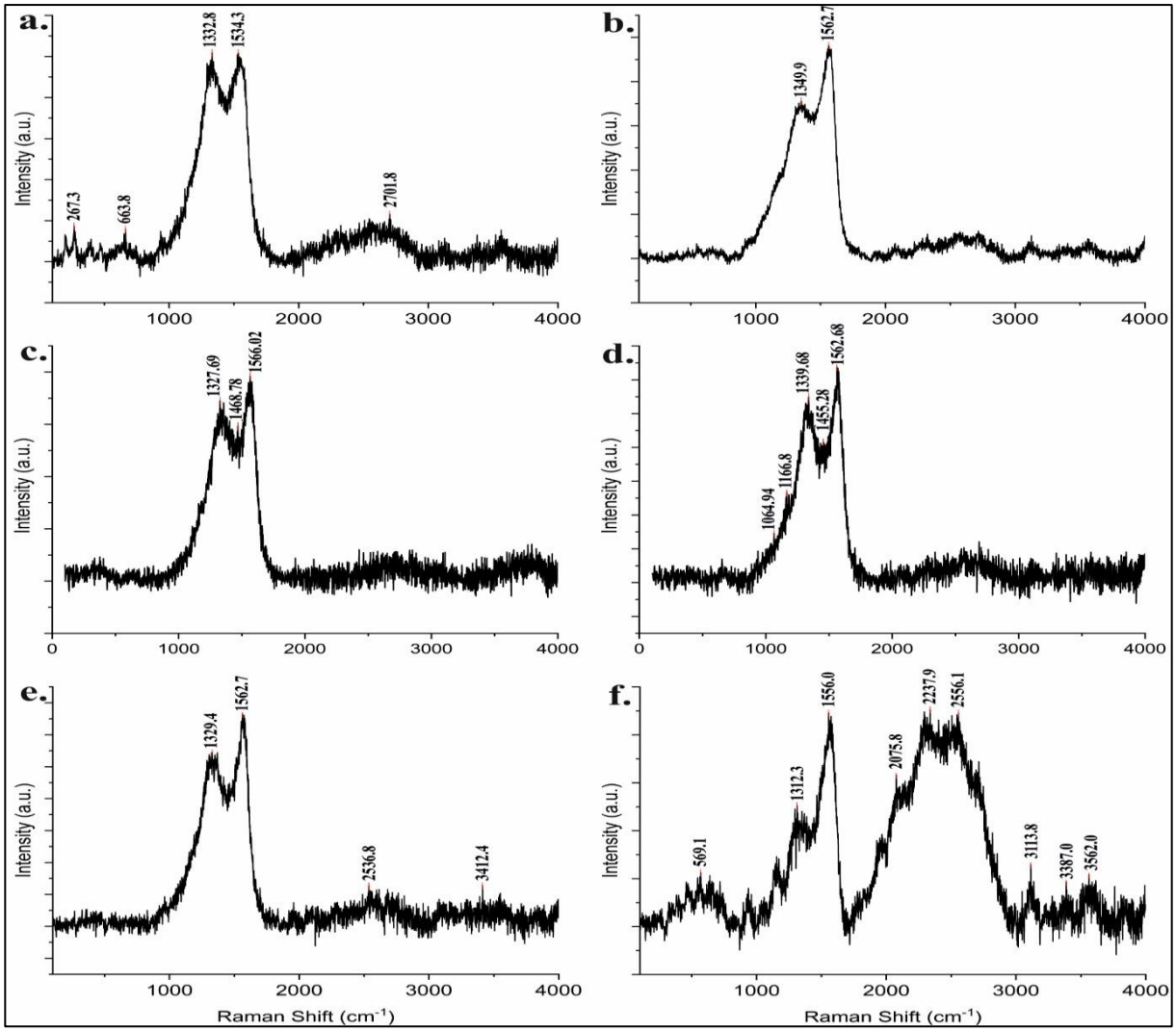

Figs. 6(a-f). Raman spectra (a-f) of aerosol samples collected in June 2020 from WIHG Campus, Dehradun

respectively (Ferrari & Robertson, 2000; Sadezky *et al.,* 2005). The narrow peak shapes and prominent intensities of these bands, especially in Figs. 6(a-e), are signatures of soot-like aerosols commonly associated with combustion sources such as vehicular and biomass burning emissions.

In Fig. 6 (a), the D and G bands appear well-defined at 1332 cm^{-1} and 1534 cm^{-1}, with a noticeable band near ~2700 cm^{-1} (2D band), suggesting layered carbon structures or more graphitized soot particles (Tuinstra F & Koenig Jl, 1970). The minor peaks at ~600-700 cm^{-1} may correspond to C-H bending or C-C skeletal vibrations from aged organic aerosol matter (Long, 2004). Fig. 6 (b) also shows a similar D-band, suggesting relatively ordered soot particles, which could result from atmospheric aging or reduced local combustion just before the monsoon. Figs. 6 (c and d) show the D- and G-bands around 1327-1355 cm^{-1} and 1550–1580 cm^{-1}, respectively. The signal broadening, especially in Fig. 6 (d), may be attributed to complex organic mixtures with photochemically processed and long-range transported material.

Fig. 6 (e) has a clearer G-band (~1562 cm^{-1}) and diminished D-band, potentially reflecting aged aerosol particles with a higher degree of graphitization. Weak bands at ~2500-3100 cm^{-1} may relate to C-H overtones or molecular vibrations from oxygenated organic aerosols. Fig. 6 (f) displays a unique spectral profile with the absence of clear D/G peaks but broad, structured bands near 1500-3000 cm^{-1}, highlighting a dominance of aliphatic C-H stretching and possibly contributions from PAHs or fossil fuel-related emissions (Movasaghi *et al.,* 2007; K. Pandey *et al.,* 2024).

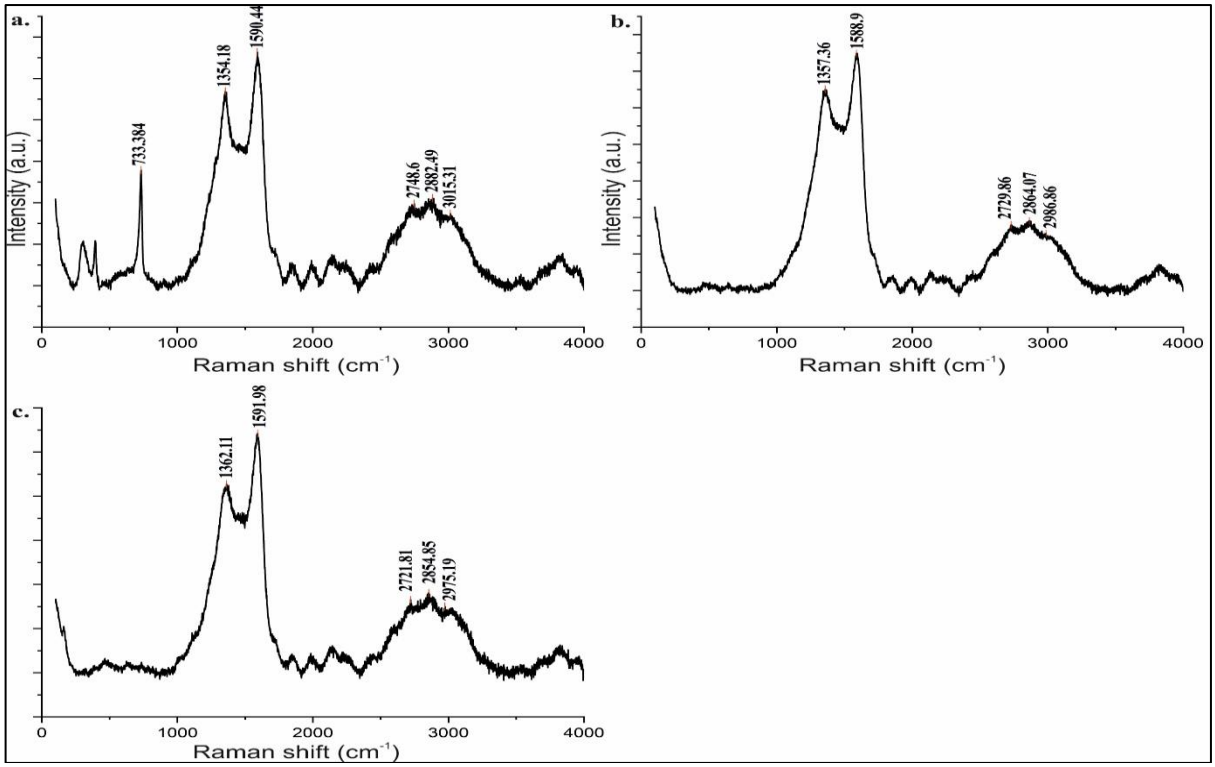

Figs. 7(a-c). Raman spectra (a-c) of aerosol samples collected in July 2020 from WIHG Campus, Dehradun

The data investigated here represents the onset of monsoon in Dehradun, suggesting a shift toward more aged, oxidized aerosols, with possible washout of coarse particles and maybe retention of fine-sized particles that originate from biomass burning activities. The variations in spectral peaks point to complex SOA formation processes and partial atmospheric removal mechanisms through precipitation.

3.2.4. *July*

The Raman spectra of aerosol samples from July 2020 (Figs. 7 (a-c) reveal signatures of carbonaceous and oxidized organic aerosols shaped by monsoonal conditions. All spectra exhibit strong D (~1350-1362 cm^{-1}) and G (~1580-1591 cm^{-1}) bands, confirming the presence of disordered and graphitic carbon typical of soot from combustion sources (Ferrari & Robertson, 2000; Sadezky *et al.,* 2005). Broader band shapes, especially in Fig. 7 (c), suggest atmospheric aging and mixing with secondary organics.

Fig. 7 (a) shows clear D and G bands, along with weaker features near 733 and ~1750 cm^{-1}, pointing to organonitrate or carbonyl groups. Broad bands in the 2748-3015 cm^{-1} region indicate aliphatic C-H stretching from long-chain hydrocarbons or HULIS (Liu *et al.,* 2016; Long, 2004). In Fig. 7 (b), the dominant G-band and overlapping peaks at 2729 and 2986 cm^{-1} suggest aging and SOA condensation (Kumar *et al.,* 2016; Movasaghi *et al.,* 2007). Fig. 7 (c) displays similar organic-rich features with strong aliphatic C-H bands at 2721, 2854, and 2975 cm^{-1}, indicative of enhanced SOA formation under humid conditions (Hinks *et al.,* 2018).

Overall, the July spectra show stronger organic signatures than previous months, reflecting monsoonal washout of coarse particles and accumulation of fine, aged aerosols. These results underscore the role of seasonal meteorology in driving aerosol aging and transformation in Himalayan environments.

3.2.5. *August*

The Raman spectra of aerosol particles collected in August 2020 (Figs. 8 (a-d)) continue to exhibit the characteristic carbonaceous signatures observed in previous months, but with distinct enhancements in oxidized and aliphatic features. In all four spectra, the dominant D-band (~1350-1380 cm^{-1}) and G-band (~1580-1610 cm^{-1}) reflect the presence of disordered (sp^3) and graphitized (sp^2) carbon structures, indicative of combustion-derived soot and related BC fractions (Ferrari & Robertson, 2000; Sadezky *et al.,* 2005).

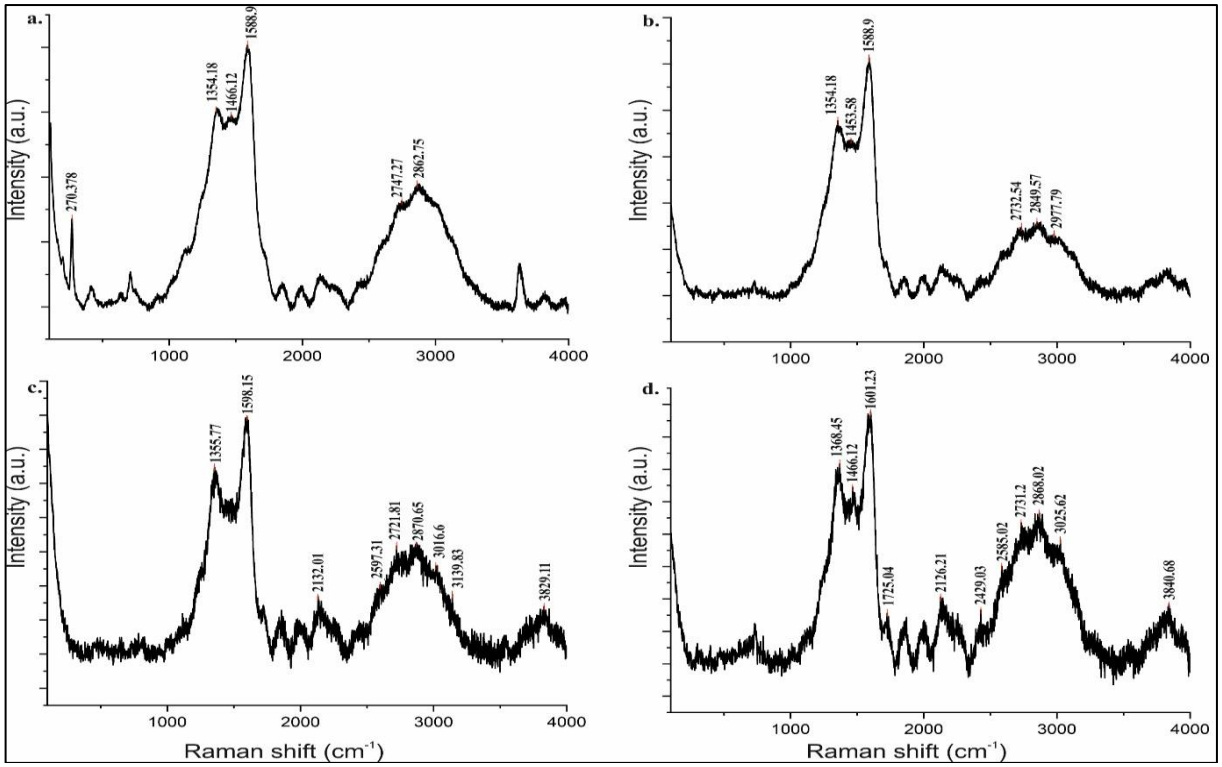

Figs. 8(a-d). Raman spectra of ambient aerosol samples from WIHG Campus, Dehradun (August 2020)

The top left and top right spectra show prominent peaks around 1466-1453 cm^{-1}, which are typically associated with C-H bending vibrations from alkyl chains, often seen in aged organic aerosol matter (Liu *et al.,* 2016; Long, 2004). These features, coupled with the sharp peak at 1588-1589 cm^{-1} (G-band), suggest the co-existence of primary carbonaceous aerosols and SOA processed under high relative humidity during the monsoon season.

Bottom panel spectra (c-d), especially (c), reveal additional complexity. The broad envelope from ~2700-3100 cm^{-1} includes overtone and combination bands, with sharp peaks at ~2721-2775, ~2870, and ~3016 cm^{-1}. These are attributed to aliphatic and aromatic C-H stretching modes, characteristic of both saturated hydrocarbons and PAHs (Kumar *et al.,* 2016; Movasaghi *et al.,* 2007). The signal broadening in this region, along with overlapping features near 2130-2150 cm^{-1} and ~2430 cm^{-1}, may result from contributions of nitrate-bearing organics or surface-bound functional groups on aged soot cores (Hinks *et al.,* 2018; Joo *et al.,* 2024).

Furthermore, the relatively enhanced Raman peaks in the fingerprint region (1250-1450 cm^{-1}) point toward an increasing share of oxidized organic material, such as HULIS or SOAs, formed through aqueous-phase oxidation during monsoon downpours and high humidity (Gopinath *et al.,* 2022; Jimenez *et al.,* 2009).

The Raman spectra from August 2020 demonstrate a shift towards a more aged and functionally complex aerosol composition, influenced by monsoonal atmospheric conditions that promote secondary processing and long-range transport.

3.2.6. *September*

The Raman spectra from September 2020 (Figs. 9 (a-c)), a transitional phase from monsoon to post-monsoon, reflect a complex mixture of carbonaceous and oxidized organic aerosol constituents. All three spectra display distinct D-bands (~1350-1380 cm^{-1}) and G-bands (~1581-1591 cm^{-1}), consistent with the signatures of soot and graphitic carbon (Ferrari & Robertson, 2000; Sadezky *et al.,* 2005). These peaks reflect a mixture of sp^2- and sp^3-hybridized carbon atoms, typical of fresh and aged combustion-related PM.

Fig. 9 (a) spectrum reveals a D-band at 1371 cm^{-1} and a G-band at 1591 cm^{-1}, along with smaller features at ~700 cm^{-1} and 1298 cm^{-1}, which may be associated with C-H bending vibrations and C-C skeletal modes, possibly from HULIS or oxygenated organic aerosols (Jimenez *et al.,*

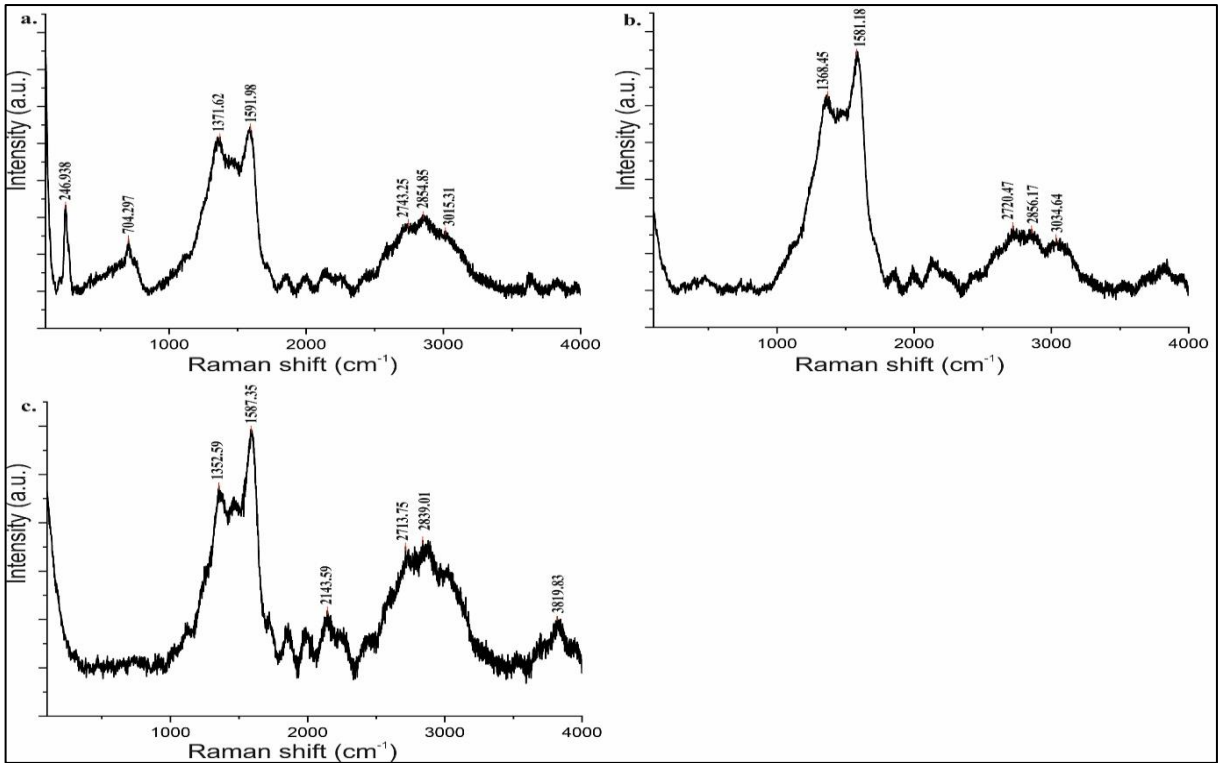

Figs. 9(a-c). Raman spectra of aerosol particles collected in September 2020 at WIHG Campus, Dehradun

2009; Long, 2004). Peaks around ~2720-2860 cm^{-1} in this spectrum are attributed to aliphatic C-H stretching, often indicative of SOA formation via photochemical aging (Liu *et al.,* 2016).

Fig. 9 (b) spectrum shows sharper and more intense D (1368 cm^{-1}) and G (1581 cm^{-1}) bands, suggesting fresh soot particles or enhanced vehicular biomass burning during drier post-monsoon days. Additionally, Raman features in the 2700-3100 cm^{-1} range (especially at ~2720, ~2856, and ~3034 cm^{-1}) correspond to symmetric and asymmetric stretching of CH_2 and CH_3 groups, pointing toward the presence of semi-volatile organics and PAHs (Kumar *et al.,* 2016; Movasaghi *et al.,* 2007).

Fig. 9 (c), with well-resolved D (1352 cm^{-1}) and G (1587 cm^{-1}) bands and overtone features at ~2713-2840 cm^{-1}, demonstrates an aged soot matrix with surface-bound oxygenated functionalities, likely due to long-range atmospheric transport and aqueous-phase oxidation during the monsoon's trailing end (Hinks *et al.,* 2018; Joo *et al.,* 2024). The feature at ~2143 cm^{-1} may indicate nitrile or cyanide groups or atmospheric nitration reactions.

Overall, the September spectra depict an aerosol system rich in combustion-generated carbon, but increasingly overlapped by secondary organic material, reflecting seasonal chemical aging and regional atmospheric dynamics during the monsoon's retreat phase.

3.2.7. *Meteorology and its relation with aerosol particles*

In this study, we have used the meteorological in-situ observations from Dehradun and Raman spectroscopic analysis of atmospheric aerosol particles during April-September 2020 at WIHG revealed significant correlations between environmental conditions and carbonaceous aerosol characteristics. As shown in Fig. 10 (a), the meteorological parameters showed typical Himalayan foothill monsoon progression, with rainfall increasing from low pre-monsoon values to peak values exceeding 600 mm during July-August, and similarity of monsoonal progression can be seen throughout the meteorological observations. Temperature ranges from 30 °C during pre-monsoon to 20-25 °C during active monsoon phases, while relative humidity depicts seasonal transitions from 60-70% to 80-90% saturation levels as precipitation increases. The I_D/I_G spectral intensity ratios, representing the degree of graphitic ordering in carbonaceous aerosols, demonstrated remarkable stability around 0.8 ± 0.1 throughout the study period despite all the meteorological variability, suggesting that the structural characteristics of atmospheric carbon particles

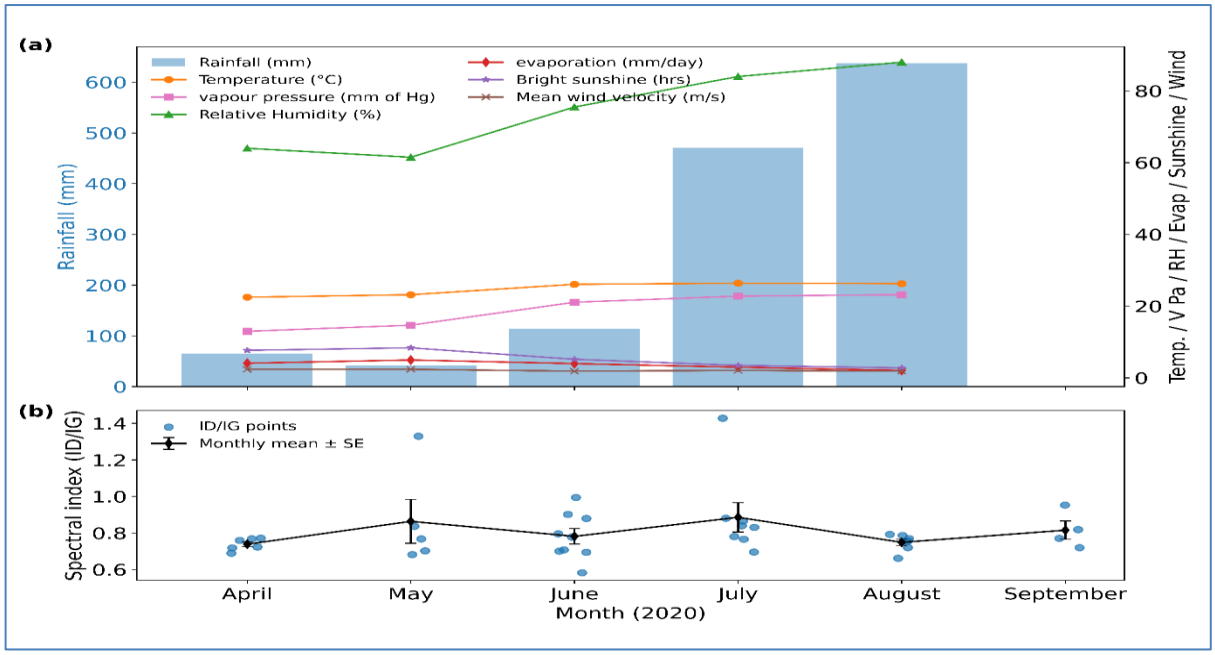

Figs. 10(a&b). (a) Monthly variability of meteorological parameters (rainfall, temperature (Temp.), vapor pressure (V Pa), relative humidity (RH), evaporation (Evap), bright sunshine (Sunshine) and wind) and (b) Raman spectroscopic I_D/I_G ratios of carbonaceous aerosols at Dehradun during April - September 2020 and monthly mean with standard error (± SE)

remained relatively constant irrespective of seasonal precipitation and humidity changes because of the restricted lockdown during COVID-19. This consistency in I_D/I_G ratios indicates that the predominant carbonaceous aerosol sources are most likely a mixture of biomass burning and fossil fuel combustion. Investigation also suggests similar combustion characteristics and aging processes during both dry and wet atmospheric conditions. The stability of I_D/I_G ratios throughout April-September 2020, during India's COVID-19 lockdowns and phased re-openings, indicates that essential combustion sources like residential biomass use and agricultural burning continued to dominate carbonaceous aerosol characteristics despite reductions in traffic and industry in the study area. The consistent atmospheric particle structure in the study area shows that everyday sources like household cooking and crop burning may continue to shape air pollution in the Himalaya, even when traffic and industries were shut down during COVID-19 lockdowns, effectively highlighting their ongoing role in regional and local air quality and climate effects.

3.2.8. *Statistical analysis*

Analysis of aerosol particles' I_D/I_G ratios during April-September 2020 (Fig. 10 (b)), 1st phase of lockdown in India, during this time, all unnecessary transportation was stopped, which has neither revealed any significant variations in the particle structure nor any carbon structure disorder. F-statistics indicating no significant monthly variation ($F(5, 33) = 0.986$, $p = 0.441$), despite reductions in all the primary emissions. The dominance of graphitic particles in the sample (69.2%, $I_D/I_G < 0.8$) and a mean I_D/I_G of 0.805 ± 0.158 shows that, even under reduced traffic and industrial emission activity, aged carbonaceous aerosol particles continued to dominate. The moderate effect size ($\eta^2 = 0.130$) indicates that monthly changes accounted for only about 13% of the variation in particle structure, while COVID-19 lockdowns and related emission reductions primarily influenced aerosol concentrations rather than their graphitic characteristics. Levene's test confirmed equal variances ($p = 0.471$), and even though two monthly groups showed slight non-normality, the ANOVA results held firm, demonstrating that lockdown-driven emission reductions did not significantly alter the carbon structure of atmospheric aerosols.

The monthly Raman spectral analysis of aerosol samples collected from the WIHG Campus in Dehradun during the COVID-19 lockdown (April-September 2020) offers comprehensive insights into the chemical evolution of atmospheric particulates across pre-monsoon, monsoon, and early post-monsoon phases in the northwestern Himalayan foothill region.

During the pre-monsoon period (April-May), strong and sharp D (1330-1350 cm^{-1}) and G (1580-1600 cm^{-1}) bands were consistently observed in almost all spectra,

indicative of freshly emitted soot-like particles from biomass burning, vehicular emissions, and domestic combustion sources (Ferrari & Robertson, 2000; Sadezky *et al.,* 2005). Secondary peaks at ~1730 cm^{-1} and ~2900 cm^{-1} further suggest the presence of carbonyl and aliphatic C-H groups, pointing toward aged organic aerosols and possible HULIS (Hinks *et al.,* 2018). These signatures reflect increased atmospheric photochemistry and accumulation of fine-mode particles typical of the dry pre-monsoon atmosphere, with limited wet scavenging.

As the region transitioned into the monsoon season (June-August), a noticeable spectral shift emerged. Although carbonaceous D and G bands persisted, they appeared relatively broadened or reduced in intensity, particularly in June and August spectra, implying partial washout of freshly emitted soot and increased aging of residual aerosols (Ram & Sarin, 2010). Elevated intensities around ~2500-3100 cm^{-1} in many spectra correspond to C-H overtone and stretching modes, suggesting enhanced organic content, likely from photochemically oxidized semi-volatile compounds (Kumar *et al.,* 2016; Liu *et al.,* 2016). Distinct peaks near 1100-1300 cm^{-1} in several July and August spectra also suggest polysaccharide-like or bioaerosol components, possibly linked to increased biological activity and moisture availability during monsoonal humidity (Pöschl, 2005). Moreover, features near 1600-1750 cm^{-1} in July-August samples underscore the buildup of oxygenated organic species, especially carbonyl and carboxylic groups consistent with in-cloud processing or aqueous-phase oxidation during long-range transport (Kampf *et al.,* 2013).

In the post-monsoon onset month of September, the spectra reveal a reemergence of sharp D and G bands, along with strong overtone features and aliphatic signals (2700-3100 cm^{-1}). This indicates a resurgence of combustion-derived aerosols, potentially due to drying of surface emissions and reduced scavenging efficiency. The spectral richness in September also suggests SOA formation from post-monsoon photochemistry, which is enhanced due to clearer skies and increased solar flux (Chakraborty *et al.,* 2018).

A study done in 2020 by (C. P. Pandey & Negi, 2022) revealed that ambient aerosols collected during May 2020 were overwhelmingly carbonaceous, with C and O comprising over 90% of observed elemental mass and trace amounts of Si, Na, Al, K, Ca, Mg, and Ti reflecting mineral dust and crustal sources. The dominance of carbon and oxygen correlates directly with the intense D (~1350 cm^{-1}) and G (~1580 cm^{-1}) Raman bands observed in these samples, confirming the prevalence of disordered and graphitic BC. Minor Raman features in the 1700-3100 cm^{-1} region attributed to C=O stretching and C-H aliphatic vibrations mirror the presence of oxygenated organic compounds suggested by the EDX oxygen-rich signature. Additionally, the fractal and aggregated morphologies seen in scanning electron microscope (SEM) align with the broadened Raman band shapes, indicating mixed aging and aggregation states of carbonaceous particles. Being our own published study, the complementary SEM-EDX and Raman data together elucidate both the elemental makeup and molecular structure of lockdown-period aerosols in the Doon Valley.Overall, the Raman spectral progression across these months reflects a clear chemical transition in aerosol composition from fresh carbonaceous emissions in the dry pre-monsoon period, to aged and oxidized organic matter during the wet monsoon, followed by a partial restoration of combustion signatures in the post-monsoon phase. This analysis, conducted during an unprecedented emission-minimized COVID lockdown period, provides a rare baseline of natural and secondary aerosol processes under relatively clean atmospheric conditions.

4. Conclusions

This study presents one of the first detailed RS investigations of atmospheric aerosol particles from Doon Valley during the COVID-19 lockdown. Monthly spectral analyses of TSP from April to September 2020 reveal distinct seasonal transitions in aerosol composition and chemistry.

Raman spectral profiles during the pre-monsoon months (April-May) were dominated by strong and well-defined D (~1330-1350 cm^{-1}) and G (~1580-1600 cm^{-1}) bands, reflecting the predominance of freshly emitted soot and carbonaceous particles from biomass burning and anthropogenic combustion sources. Additional bands in the ~1730 cm^{-1} and ~2900 cm^{-1} regions suggested contributions from oxygenated organic compounds and HULIS, typical of aged or secondary aerosols.

During the monsoon period (June-August), a notable shift in spectral features was observed. The D and G bands persisted but with reduced sharpness and intensity, likely due to atmospheric aging, wet scavenging, and long-range transport. Prominent signals corresponding to aliphatic and oxygenated functional groups indicated enhanced photochemical processing and aqueous-phase reactions under high humidity and cloud cover. In particular, July and August spectra reflected a richer organic aerosol matrix, suggesting the buildup of SOAs through in-cloud and aqueous-phase oxidation.

In the post-monsoon onset (September), spectral characteristics indicated a resurgence of combustion-derived carbonaceous material, coupled with retained features of oxidized organics. This points to the resumption of local emissions and decreased atmospheric cleansing.

The analysis reveals that despite substantial reductions in emissions during the lockdown, the structural characteristics of carbonaceous aerosols remained largely unchanged. This suggests that long-range transport and the dominance of aged graphitic particles played a stronger role than local emission reductions in shaping aerosol structure.

4.1. *Limitations*

Despite providing valuable insights, this study has certain limitations. Seasonal variation could not be fully assessed, as a larger dataset would be required to establish statistically robust conclusions. Furthermore, various elemental analyses, such as Scanning Electron Microscopy - Energy Dispersive X-ray analysis and X-Ray Diffraction, would have strengthened the chemical characterization of aerosols. However, due to constraints of time and limited sample availability, these aspects could not be undertaken in the present work.

Overall, the study demonstrates the capability of RS in characterizing the chemical heterogeneity of aerosol particles and tracing their seasonal evolution. The results also provide a critical baseline for future assessments of aerosol transformation processes in high-altitude pristine environments, especially under low-emission conditions. These findings highlight the interplay between local sources, atmospheric processing, and meteorology in governing aerosol composition over the Himalayan foothills.

Data availability

The datasets generated and/or analyzed during the current study are not publicly available, but are available from the corresponding author on reasonable request.

Funding

This work is supported by Activity 4, Wadia Institute of Himalayan Geology, Dehradun, and Aman Shrivas is funded by the SERB project number CRG/2023/001900.

Conflict of Interest: The authors declare that they have no conflict of interest.

Authors' statement

The authors declare that the work presented in this manuscript is original and has not been published elsewhere, nor is it currently under consideration for publication by any other journal. All authors have significantly contributed to the research and preparation of the manuscript. They have read and approved the final version and agree to be accountable for all aspects of the work in ensuring that questions related to the accuracy or integrity of any part of the work are appropriately investigated and resolved.

Acknowledgement

The authors sincerely thank the Director of the Wadia Institute of Himalayan Geology (WIHG**)**, Dehradun, for providing the necessary facilities and support to carry out this research. AS would like to thank the SERB CRG/2023/001900 project for providing a fellowship to conduct this research. AT, PS would like to thank UGC, SR to CSIR for granting fellowship to conduct this research.

Authors' Contributions

Aman Shrivas: Conceptualzation, Methodoloy, Formal analysis, Investigation, Writing – Original Draft and Writing – Review & Editing.
Chhavi Pant Pandey: Conceptualzation, Methodoloy, Investigation, Writing – Original Draft, Writing – Review & Editing and Supervision.
Abhishek Thakur: Formal analysis, Writing – Original Draft and Writing – Review & Editing.
Parakh Sahu: Methodoloy, Investigation and Writing – Review & Editing.
Swarnedu Roy: Methodoloy, Formal analysis, Investigation and Writing – Review & Editing.

Disclaimer: The contents and views presented in this research article/paper are the views of the authors and do not necessarily reflect the views of the organizations they belong to.

Reference

Asrafali, S. P., Periyasamy, T., Kim, S. C., and Lee, J. W., 2024, "Enhanced Wettability and Adhesive Property of PTFE through Surface Modification with Fluorinated Compounds", *Materials*, **17,** 13, doi : https://doi.org/10.3390/ma17133051.

Bond, T. C., Doherty, S. J., Fahey, D. W., Forster, P. M., Berntsen, T., Deangelo, B. J., Flanner, M. G., Ghan, S., Kärcher, B., Koch, D., Kinne, S., Kondo, Y., Quinn, P. K., Sarofim, M. C., Schultz, M. G., Schulz, M., Venkataraman, C., Zhang, H., Zhang, S., Zender, C. S., 2013, "Bounding the role of black carbon in the climate system: A scientific assessment", *Journal of Geophysical Research Atmospheres*, **118**, 5380–5552. https://doi.org/10.1002/jgrd.50171.

Buckner, C. A., Lafrenie, R. M., Dénommée, J. A., Caswell, J. M., Want, D. A., Gan, G. G., Leong, Y. C., Bee, P. C., Chin, E., Teh, A. K. H., Picco, S., Villegas, L., Tonelli, F., Merlo, M., Rigau, J., Diaz, D., Masuelli, M., Korrapati, S., Kurra, P., … Mathijssen, R. H. J., 2016, "We are IntechOpen , the world ' s leading publisher of Open Access books Built by scientists , for scientists TOP 1 %", *Intech*, **11**(tourism), 13. https://www.intechopen.com/books/advanced-biometric-technologies/liveness-detection-in-biometrics.

Chakraborty, A., Mandariya, A. K., Chakraborti, R., Gupta, T., and Tripathi, S. N., 2018, "Realtime chemical characterization of post monsoon organic aerosols in a polluted urban city: Sources, composition, and comparison with other seasons", *Environmental Pollution*, **232**, 310–321, doi: https://doi.org /10.1016/j.envpol.2017.09.079.

Chandrakala, M., Nandan, R., Ratnam, M. V., and Bhaskara Rao, S. V. 2024, "Source apportionment of black carbon and the impact of COVID-19 lockdown over a semi-urban location in India", *Atmospheric Environment: X*, **21**(October 2023), 100243, doi: https://doi.org/10.1016/j.aeaoa.2024.100243

Cheng, Y. H., and Lin, M. H., 2013, "Real-time performance of the microaeth® AE51 and the effects of aerosol loading on its measurement results at a traffic site", *Aerosol and Air Quality Research*, **13,** 6, 1853-1863, doi: https://doi.org/ 10.4209/aaqr. 2012.12.0371

Chin, M., Diehl, T., Bian, H. and Kucsera, T., 2015, "Aerosols in the atmosphere: Sources, transport, and multi-decadal trends", Paper presented at *34th International Technical Meeting on Air Pollution Modelling and its Applications (ITM)*, Montpellier, France, 4-8 May. NASA Technical Report GSFC-E-DAA-TN22950.https://ntrs.nasa.gov/citations/20200002834[Accessed 12 September 2025].

Contini, D., Vecchi, R., and Viana, M., 2018), "Carbonaceous aerosols in the atmosphere", *Atmosphere*, **9,** 5, 1–8, doi: https://doi.org/ 10.3390/atmos9050181.

Deep, A., Pandey, C. P., Nandan, H., Purohit, K. D., Singh, N., Singh, J., Srivastava, A. K., and Ojha, N., 2019, "Evaluation of ambient air quality in Dehradun city during 2011–2014", *Journal of Earth System Science*, **128,** 4, 1–14, doi: https://doi.org/10.1007 /s12040-019-1092-y.

Dhankar, S., Singh, G., & Kumar, K., 2024, "Impacts of urbanization on land use, air quality, and temperature dynamics in Dehradun district of Uttarakhand, India: a comprehensive analysis", *Frontiers in Environmental Science*, **12,** (February), 1–15, doi: https://doi.org/10.3389/fenvs.2024.1324186.

Doughty, D. C., and Hill, S. C., 2020, "Raman spectra of atmospheric aerosol particles: Clusters and time-series for a 22.5 hr sampling period", *Journal of Quantitative Spectroscopy and Radiative Transfer*, **248**, 106907, doi: https://doi.org/10.1016 /j.jqsrt.2020.106907.

Estefany, C., Sun, Z., Hong, Z., and Du, J., 2023, "Raman spectroscopy for profiling physical and chemical properties of atmospheric aerosol particles: A review", *Ecotoxicology and Environmental Safety*, **249,** (December 2022), doi: https://doi.org/10.1016/ j.ecoenv.2022.114405.

Ferrari, A. C., and Robertson, J., 2000, "Interpretation of Raman spectra of disordered and amorphous carbon", *Physical Review B*, **61,** 20, 14095–14107, doi: https://doi.org/10.1103/PhysRev B.61.14095.

Gopinath, A. K., Raj, S. S., Kommula, S. M., Jose, C., Panda, U., Bishambu, Y., Ojha, N., Ravikrishna, R., Liu, P. and Gunthe, S. S. (2022), "Complex Interplay Between Organic and Secondary Inorganic Aerosols With Ambient Relative Humidity Implicates the Aerosol Liquid Water Content Over India During Wintertime", *Journal of Geophysical Research: Atmospheres*, **127,** 13, doi: https://doi.org/10.1029/2021JD036430.

Government of Uttarakhand., 2018, Human development report of Uttarakhand 1–357.

Hinks, M. L., Montoya-Aguilera, J., Ellison, L., Lin, P., Laskin, A., Laskin, J., Shiraiwa, M., Dabdub, D., and Nizkorodov, S. A. 2018, "Effect of relative humidity on the composition of secondary organic aerosol from the oxidation of toluene", *Atmospheric Chemistry and Physics*, **18,** 3, 1643–1652, doi: https://doi.org/10.5194/acp-18-1643-2018.

Ivleva, N. P., Messerer, A., Yang, X., Niessner, R., and Pöschl, U., 2007, "Raman microspectroscopic analysis of changes in the chemical structure and reactivity of soot in a diesel exhaust aftertreatment model system", *Environmental Science and Technology*, **41,** 10, 3702–3707, doi: https://doi.org/10.1021/es0612448.

Jacobson, M.C., Hansson, H.C., Noone, K.J. and Charlson, R. J., 2000, "Organic atmospheric aerosols: Review and state of the science", *Reviews of Geophysics*, **38,** 2, 267–294, doi: https://doi.org/10.1029/1998RG000045.

Jimenez, J. L., Canagaratna, M. R., Donahue, N. M., Prevot, A. S. H., Zhang, Q., Kroll, J. H., DeCarlo, P. F., Allan, J. D., Coe, H., Ng, N. L., Aiken, A. C., Docherty, K. S., Ulbrich, I. M., Grieshop, A. P., Robinson, A. L., Duplissy, J., Smith, J. D., Wilson, K. R., Lanz, V. A., … Worsnop, D. R., 2009, "Evolution of organic aerosols in the atmosphere", *Science*, **326**, 5959, 1525–1529, doi: https://doi.org/10.1126/science .1180353.

Joo, T., Machesky, J. E., Zeng, L., Hass-Mitchell, T., Weber, R. J., Gentner, D. R. and Ng, N. L., 2024, "Secondary Brown Carbon Formation From Photooxidation of Furans From Biomass Burning", *Geophysical Research Letters*, **51,** 1, doi: https://doi. org/10.1029/2023GL104900.

Kampf, C. J., Waxman, E. M., Slowik, J. G., Dommen, J., Pfaffenberger, L., Praplan, A. P., Prévoît, A. S. H., Baltensperger, U., Hoffmann, T., & Volkamer, R., 2013, "Effective Henry's law partitioning and the salting constant of glyoxal in aerosols containing sulfate", *Environmental Science and Technology*, **47**, 9, 4236–4244, doi: https://doi.org/10.1021/es400083d.

Kumar, B., Chakraborty, A., Tripathi, S. N., and Bhattu, D., 2016, "Highly time resolved chemical characterization of submicron organic aerosols at a polluted urban location", *Environmental Science: Processes and Impacts*, **18,** 10, 1285–1296, doi : https://doi. org/10.1039/c6em00392c.

Li, F., Li, Z., Wang, Y., Wang, S., Wang, X., Sun, C., and Men, Z., 2018, "A Raman spectroscopy study on the effects of intermolecular hydrogen bonding on water molecules absorbed by borosilicate glass surface", *Spectrochimica Acta - Part A: Molecular and Biomolecular Spectroscopy*, **196**, 317–322, doi: https://doi.org/ 10.1016/j.saa.2018.02.037.

Liu, J., Lin, P., Laskin, A., Laskin, J., Kathmann, S. M., Wise, M., Caylor, R., Imholt, F., Selimovic, V. and Shilling, J. E., 2016, "Optical properties and aging of light-absorbing secondary organic aerosol", *Atmospheric Chemistry and Physics*, **16,** 19, 12815–12827, doi : https://doi.org/10.5194/acp-16-12815-2016.

Long, D. A., 2004, "Infrared and Raman characteristic group frequencies. Tables and charts", *Journal of Raman Spectroscopy*, **35,** 10, 905–905, doi : https://doi.org/10. 1002/jrs.1238.

Mani, A., Kumari, M. and Badola, R., 2024, "Analysing Temporal and Seasonal Climate Trends in the Doon Valley, Uttarakhand", *8th International Electronic Conference on Water Sciences*, **14–16** October 2024, MDPI.

McMillan, P.F. and Wolf, G.H., 1990, "Vibrational spectroscopy of silicate liquids", *Vibrational Spectroscopy of Silicate Liquids*. Chichester: John Wiley & Sons, Chapter **8**.

McMillan, P., and Piriou, B., 1983, "Raman spectroscopic studies of silicate and related glass structure: a review", *Bulletin de Mineralogie*, **106,** 1–2, 57–75, doi : https://doi.org/10.3406/ bulmi.1983.7668.

Movasaghi, Z., Rehman, S., and Rehman, I. U., 2007, "Raman spectroscopy of biological tissues", *Applied Spectroscopy Reviews*, **42,** 5, 493-541, doi : https://doi.org/10.1080/05704920701551530.

Pandey, C. P., and Negi, P. S., 2022, "Characteristics of equivalent black carbon aerosols over Doon Valley in NW Indian Himalaya during COVID-19 lockdown 2020", *Environmental Monitoring and Assessment*, **194**, 3, doi : https://doi.org/10.1007/s10661-022-09879-9.

Pandey, K., Mishra, S. K., Singh, B. P., Khare, M., Sharma, S. K., Chandra Pandey, A., Devi, M., and Ahlawat, A., 2024, "Insights into chemical aging of urban aerosols over Delhi, India", *Atmospheric Environment: X*, **24**, September, 100296, doi : https://doi.org/10.1016/j.aeaoa.2024.100296.

Panikkar, S. V., and Subramanyan, V., 1996, "A geomorphic evaluation of the landslides around Dehradun and Mussoorie, Uttar Pradesh, India", *Geomorphology*, **15,** 2, 169-181, doi : https://doi.org/10.1016/0169-555X(95)00121-K.

Perumpully, S. J., and Gautam, S., 2024, "Impact of aerosols on atmospheric processes and climate variability: A synthesis of recent research findings" *Geosystems and Geoenvironment*, **4**, 1, 100317, doi: https://doi.org/10.1016/j.geogeo.2024.100317

Petzold, A., Ogren, J. A., Fiebig, M., Laj, P., Li, S. M., Baltensperger, U., Holzer-Popp, T., Kinne, S., Pappalardo, G., Sugimoto, N., Wehrli, C., Wiedensohler, A., & Zhang, X. Y. (2013), "Recommendations for reporting black carbon measurements", *Atmospheric Chemistry and Physics*, **13,** 16, 8365-8379, doi : https://doi.org/10.5194/ACP-13-8365-2013.

Piyoosh, A. K., and Ghosh, S. K., 2016, "A comparative assessment of temperature data from different sources for Dehradun, Uttarakhand, India", *Journal of Meteorological Research*, **30,** 6, 1019–1032, doi : https://doi.org/10.1007/s13351-016-6031-0.

Pöschl, U., 2005, "Atmospheric aerosols: Composition, transformation, climate and health effects", *Angewandte Chemie - International Edition*, **44,** 46, 7520–7540, doi : https://doi.org/10.1002/anie.200501122.

Ram, K., & Sarin, M. M., 2010, "Spatio-temporal variability in atmospheric abundances of EC, OC and WSOC over Northern India", *Journal of Aerosol Science*, **41,** 1, 88-98, doi : https://doi.org/10.1016/j.jaerosci.2009.11.004.

Ramachandran, S., Rupakheti, M., Cherian, R., and Lawrence, M. G. 2023, "Aerosols heat up the Himalayan climate", *Science of the Total Environment*, **894**, June, 164733, doi: https://doi.org/10.1016/j.scitotenv.2023.164733.

Rao, C. N. R., 1978, "Raman Spectra of Complex Metal Oxides", *Indian Journal of Pure and Applied Physics*, **16**, 3, 277–281.

S, S. A., D, M. S., Tushar, K., Jai, K., and A, B. S., 2013, "Influence of Atmospheric Aerosols on Health and Environment-Climate Environment-Climate Change", *International Journal of Life Sciences*, April, 115-120.

Sadezky, A., Muckenhuber, H., Grothe, H., Niessner, R., and Pöschl, U. 2005, "Raman microspectroscopy of soot and related carbonaceous materials: Spectral analysis and structural information", *Carbon*, **43,** 8, 1731-1742, doi : https://doi.org/10.1016/j.carbon.2005.02.018.

Sangkham, S., Phairuang, W., Sherchan, S. P., Pansakun, N., Munkong, N., Sarndhong, K., Islam, M. A., & Sakunkoo, P., 2024, "An update on adverse health effects from exposure to PM2.5", *Environmental Advances*, **18,** September, p100603, doi : https://doi.org/10.1016/j.envadv.2024.100603.

Sedlacek, A. J., 2016, "Aethalometer™ Instrument Handbook", *U.S. Department of Energy*, *DOE/SC-ARM* (April), 1-28, https://www.arm.gov/publications/tech_reports/handbooks/aeth_handbook.pdf.

Sharma, A., Bhattacharya, A., and Venkataraman, C., 2022, "Influence of aerosol radiative effects on surface temperature and snow melt in the Himalayan region", *Science of the Total Environment*, **810**, 151299, doi : https://doi.org/10.1016/j.scitotenv. 2021.151299.

Shrivas, A., and Pandey, C. P., 2024, "Optical and Physico-chemical Characteristics of Ambient Aerosols Along Gangotri Glacier Valley in Western Himalaya, India", *Aerosol Science and Engineering*, doi : https://doi.org/10.1007/s41810-024-00264-2.

Singh, O., Arya, P., and Chaudhary, B. S., 2013, "On rising temperature trends at Dehradun in Doon valley of Uttarakhand, India", *Journal of Earth System Science*, **122,** 3, 613-622, doi : https://doi.org/10.1007/s12040-013-0304-0.

Sinha, S., & Sinha, R., 2016, "Geomorphic evolution of Dehra Dun, NW Himalaya: Tectonics and climatic coupling", *Geomorphology*, **266**, 20-32, doi : https://doi.org/10.1016/ j.geomorph.2016.05.002.

Sobanska, S., Falgayrac, G., Rimetz-Planchon, J., Perdrix, E., Brémard, C., and Barbillat, J., 2014, "Resolving the internal structure of individual atmospheric aerosol particle by the combination of Atomic Force Microscopy, ESEM-EDX, Raman and ToF-SIMS imaging", *Microchemical Journal*, **114**, 89-98, doi: https://doi.org/10.1016/j.microc.2013.12.007.

Tuinstra F. and Koenig Jl., 1970, "Raman Spectrum of Graphite", *Journal of Chemical Physics*, **53,** 3, 1126-1130, doi : https://doi.org/10.1063/1.1674108.

Van Poppel, M., Peters, J., Levei, E. A., Mărmureanu, L., Moldovan, A., Hoaghia, M. A., Varaticeanu, C., and Van Laer, J., 2023, "Mobile measurements of black carbon: Comparison of normal traffic with reduced traffic conditions during COVID-19 lock-down", *Atmospheric Environment*, **297,** November 2022, doi : https://doi.org/10.1016/j.atmosenv.2023.119594.

Verma, R. L., and Kamyotra, J. S., 2021, "Impacts of COVID-19 on air quality in India", *Aerosol and Air Quality Research*, **21,** 4, 4025–4037, doi : https://doi.org/10.4209/aaqr.200482.

Watson, J. G., Chow, J. C., and Chen, L.-W. A., 2005, "Summary of Organic and Elemental Carbon/Black Carbon Analysis Methods and Intercomparisons", *Aerosol and Air Quality Research***, 5**, 1, doi : https://doi.org/10.4209/aaqr.2005.06.0006.

Watson, J. G., Chow, J., Frank, N., and Homolya, J., 1998, "Guideline on speciated particulate monitoring, Draft 3", *Desert Research Institute*, August, **291**, epa.gov/ttnamti1/files/ambient/pm25/spec/drispec.pdf.

Yan, C., Zheng, M., Shen, G., Cheng, Y., Ma, S., Sun, J., Cui, M., Zhang, F., Han, Y. and Chen, Y., 2019, "Characterization of carbon fractions in carbonaceous aerosols from typical fossil fuel combustion sources", *Fuel*, **254,** March, 115620, doi : https://doi.org/10.1016/j.fuel.2019.115620.

Zhou, Q., Pang, S. F., Wang, Y., Ma, J. B., and Zhang, Y. H., 2014, "Confocal raman studies of the evolution of the physical state of mixed phthalic acid/ammonium sulfate aerosol droplets and the effect of substrates" *Journal of Physical Chemistry B*, **118,** 23, 6198-6205, doi : https://doi.org/10.1021/jp5004598.